

Frequency Response of Water Columns of Liquid Piston Stirling Engine Under No Load Condition

Arturo Mariano Isip FIGUEROA¹, Takasuke YAMASAKI², Shinichi KAMIYAMA³,
and Shinji OKAYAMA¹

¹*Chair of Plant and Animal Production Under Structure The United Graduate School of Agricultural Sciences, Ehime University ;* ²*Chair of Maritime Environmental Engineering, Faculty of Agriculture ;*

³*Institute of Fluid Science, Tohoku University*

Abstract : The frequency response of water columns in liquid piston stirling engine under no load condition is obtained theoretically by using linearized technique to our introduced nonlinear differential equation in the previous report which cannot be applied to theoretical estimation with unknown initial condition. The amplitude ratio of each water level and its phase lag and natural frequency are obtained theoretically. The results agree well with experiments.

Key words : Stirling Engine, Frequency Response, Linearization Oscillatory Flow

1 Introduction

The liquid piston stirling engine known as the Fluidyne was invented more than two decades ago and since then, many studies have been conducted to explore and describe the potential of this machine for a wide variety of applications¹⁾. The merits of this engine are obvious in terms of low cost, simplicity in construction, maintenance free, and ability to use low grade fuels²⁾.

In our previous studies concerning a feedback type liquid piston stirling engine, firstly, we introduced the basic equation of motion of the water columns and confirmed by experiments³⁾. Secondly, we investigated the direct usage of this engine to pumping water and found out its very low characteristics. This led us to the development of a new water-hammer type of pump with a remarkable output performance⁴⁾. Thirdly, we also clarified the vibration mechanism by using linear stability analysis without taking into account the friction loss terms in the introduced equation because of their very small magnitudes.

The purpose of this present work is to clarify by theoretical treatments, the frequency response about this engine system by application of linearized technique to our nonlinear differential equation, taking into account the small nonlinear friction terms (\dot{x}_n , \dot{x}_{pw} , etc.). These friction terms cannot be neglected because they play an important role in obtaining phase lag necessary for estimating engine power performance in design. We note further that our nonlinear differential equation cannot be used directly in theoretical estimation with unknown initial conditions. Hence, in this present treatment, we can obtain the useful

system function with the application of equivalent treatments ($c\dot{x}$) to various pipeline friction, not only to straight pipe, but also to convergent-divergent ducts. We confirmed these estimations by experiments.

2 Nomenclature

A	cross-sectional area
G	frequency transfer function
P	pressure
P	Fourier transformation of pressure
X	Fourier transformation of displacement
x	displacement
\dot{x}	velocity
\ddot{x}	acceleration
ρ	density
ω	angular frequency
subscript	
g	gas
l	liquid
co	cold space
he	hot space
pw	output column

3 Theoretical Procedure

Consider the engine system as shown in Fig.1(a)³⁾. From our previous equations³⁾, we cannot obtain the frequency response especially the amplitude ratio and phase lag if the friction loss is neglected. Another point to consider is that the equation cannot be used for estimation without experimental initial condition. And so in this present analysis, we take into account of friction loss inspite of having small values, to improve these fundamental equations and become useful form for characteristics estimation.

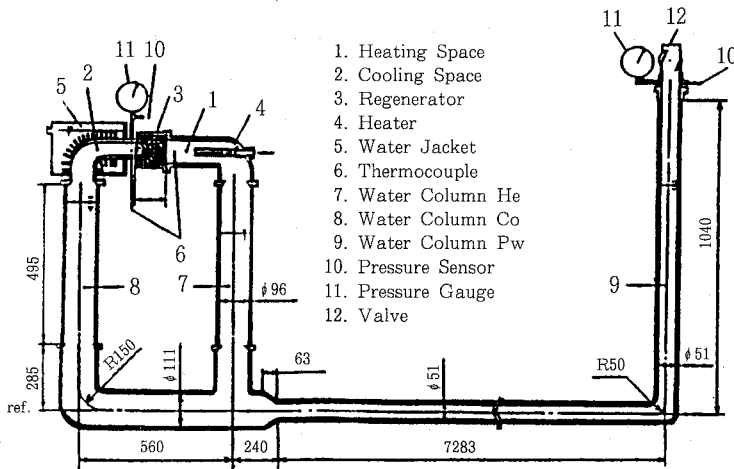
Assuming at the steady operating condition of motion that each water column might have small vibration amplitude, the friction terms can be treated as $c\dot{x}^{5-6)}$. Then the linearized equations of motion (1), (2), and continuity (3) based on our previous equations³⁾ are written as follows :

$$a_{he} \ddot{x}_{he} + b_{he} \ddot{x}_{pw} + 2c_h' \dot{x}_{he} + 2d_h' \dot{x}_{pw} + f_{he} x_{he} + i_{he} x_{he} = 0 \quad (1)$$

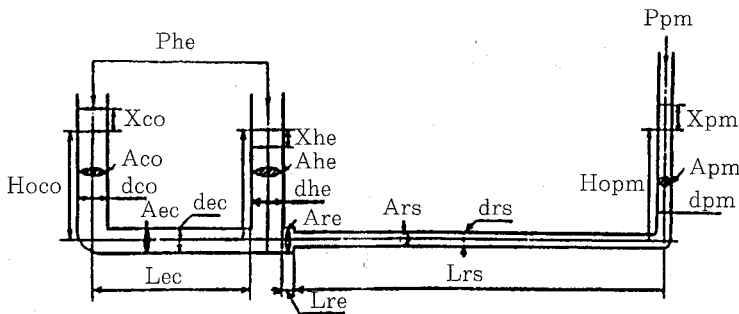
$$a_{pw} \ddot{x}_{he} + b_{pw} \ddot{x}_{pw} + (c_p' + c_h' e_{pw} / e_{he}) \dot{x}_{he} + (d_p' + d_h' e_{pw} / e_{he}) \dot{x}_{pw} + f_{pw} x_{he} + i_{pw} x_{pw} = L_p (P_{he} - P_{pw}) \quad (2)$$

$$A_{pw} x_{pw} + A_{he} x_{he} + A_{co} x_{co} = 0 \quad (3)$$

where $L_p = A_{co}^2 A_{pw} / \rho$, and the coefficients c_h' , d_h' , c_p' , and d_p' are defined as the



(a)



(b)

Fig. 1. Schematic (a) and analytic (b) diagram of the engine

approximate equivalent linear friction coefficients and the form of their frequency response are written as follows⁵⁻⁶⁾ :

$$c_h' = c_{he} \omega x_{he}^* \Psi \tag{4}$$

$$d_h' = d_{he} \omega x_{pw}^* \Psi \tag{5}$$

$$c_p' = c_{pw} \omega x_{he}^* \Psi \tag{6}$$

$$d_p' = d_{pw} \omega x_{pw}^* \Psi \tag{7}$$

where $\Psi = 8 / (3\pi)$ and the coefficients a_{he} , b_{he} , c_{he} , d_{he} , e_{he} , f_{he} , i_{he} , a_{pw} , b_{pw} , c_{pw} , d_{pw} , e_{pw} , f_{pw} , and i_{pw} are defined as constants whose magnitudes are determined by equating to zero the displacement variables x_{he} and x_{pw} inside each coefficient's expression³⁾.

Moreover, x_{he}^* and x_{pw}^* are the amplitude of oscillation at the hot space and output columns, and ω the frequency of oscillation.

Next, P_{he} is the pressure of the working gas at the heat space and P_{pw} is the load pressure at the output column and assumed of the form,

$$p_{pw} = \frac{1}{2} \rho_g C_{pp} | \dot{x}_{pw} | \dot{x}_{pw} \quad (8)$$

where C_{pp} is defined as the loss coefficient at the load side.

By linearizing p_{pw} , we get

$$p_{pw} = \frac{1}{2} \rho_g C_{pp} x_{pw}^* \omega \Psi \dot{x}_{pw} \quad (9)$$

where C_{pp} is the approximate linear damping coefficient.

Equations (1)–(3) are then Fourier transformed, which results in the following equations,

$$(f_{he} - a_{he} \omega^2 + 2c_{he} x_{he}^* \omega^2 j \Psi) X_{he} + (i_{he} - b_{he} \omega^2 + 2d_{he} x_{pw}^* \omega^2 j \Psi) X_{pw} = 0 \quad (10)$$

$$\{f_{pw} - a_{pw} \omega^2 + (c_{pw} + e_{pw} c_{he}/e_{he}) x_{he}^* \omega^2 j \Psi\} X_{he} + \{i_{pw} - b_{pw} \omega^2 + (d_{pw} + e_{pw} d_{he}/e_{he} + 0.5L_p C_{pp}) x_{pw}^* \omega^2 j \Psi\} X_{pw} = L_p P_{he} \quad (11)$$

By substituting equation (10) into equation (11), we get the characteristic equation as,

$$\begin{aligned} & \{b_{he} a_{pw} - b_{pw} a_{he}\} s^4 + \{b_{he} L_2 - a_{he} L_4 + L_1 a_{pw} - L_3 b_{pw}\} s^3 \\ & + \{i_{he} a_{pw} - f_{he} b_{pw} + b_{he} f_{pw} - a_{he} i_{pw} + L_1 L_2 - L_3 L_4\} s^2 \\ & + \{i_{he} L_2 - f_{he} L_4 + L_1 f_{pw} - L_3 i_{pw}\} s \\ & + \{i_{he} f_{pw} - i_{pw} f_{he}\} = 0 \end{aligned} \quad (12)$$

where

$$L_1 = 2d_{he} x_{he}^* \Psi \omega \quad (13)$$

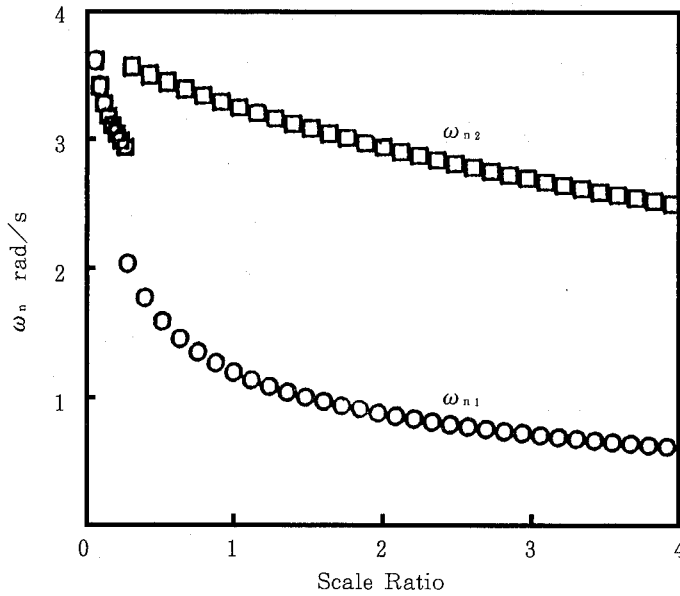
$$L_2 = (c_{pw} + e_{pw} c_{he}/e_{he}) x_{he}^* \Psi \omega \quad (14)$$

$$L_3 = 2c_{he} x_{he}^* \Psi \omega \quad (15)$$

$$L_4 = (d_{pw} + e_{pw} d_{he}/e_{he} + 0.5L_p C_{pp}) x_{pw}^* \Psi \omega \quad (16)$$

The imaginary parts of the characteristic roots of equation (12) constitute the frequency of self-excited vibration of this system. As an example of the relation of this natural frequency in equation (12) to scale ratio is shown in Fig. 2, where the scale ratio means the ratio between the dimensions (diameter and pipe length) of a similar configuration engine with the model engine in Fig.1(a).

Finally, by using equations (1),(2),(3), and (9), we obtain the frequency transfer functions of the system


 Fig. 2. Relation of natural frequency ω_n to scale ratio

$$X_{pw} / X_{he} \equiv G_{pho} = L_p(R_2 + I_2 j) / (R_3 + I_3 j) \quad (17)$$

$$X_{pw} / P_{he} \equiv G_s = L_p(R_2 + I_2 j) / (Z_1 + Z_2 j) \quad (18)$$

$$X_{he} / P_{he} \equiv G_c = L_p(R_3 + I_3 j) / (Z_1 + Z_2 j) \quad (19)$$

$$X_{co} / X_{pw} \equiv G_y = (R_5 + I_5 j) / (R_2 + I_2 j) \quad (20)$$

$$X_{co} / X_{he} \equiv G_p = (R_5 + I_5 j) / (R_3 + I_3 j) \quad (21)$$

$$X_{co} / P_{he} \equiv G_z = L_p(R_5 + I_5 j) / (Z_1 + Z_2 j) \quad (22)$$

where

$$Z_1 = R_1 R_3 - I_1 I_3 + R_2 R_4 - I_2 I_4 \quad (23)$$

$$Z_2 = R_1 I_3 + R_3 I_1 + R_4 I_2 + R_2 I_4 \quad (24)$$

$$R_1 = f_{pw} - a_{pw} \omega^2 \quad (25)$$

$$R_2 = f_{he} - a_{he} \omega^2 \quad (26)$$

$$R_3 = b_{he} \omega^2 - i_{he} \quad (27)$$

$$R_4 = i_{pw} - b_{pw} \omega^2 \quad (28)$$

$$R_5 = -(A_{pw} / A_{co} R_2 + A_{he} / A_{co} R_3) \quad (29)$$

$$I_1 = L_2 \quad (30)$$

$$I_2 = L_3 \quad (31)$$

$$I_3 = -L_1 \quad (32)$$

$$I_4 = L_4 \quad (33)$$

$$I_5 = -(A_{pw} / A_{co} I_2 + A_{he} / A_{co} I_3) \quad (34)$$

4 Experimental Procedure

The experimental engine as shown in Fig.1(a) was partly made of acrylic transparent pipe 96 mm in diameter at the hot and cold space and 51 mm at the output column to observe the oscillations of the water columns and the displacement was recorded using video camera. A stainless steel wool weighing 100 g (0.2 mm in diameter) was used as regenerator material inside a casing 90 mm in diameter and 100 mm in length. Thermocouples were embedded at the walls of the hot and cold space to measure the operating temperatures. A 0.38 kw sheath heater was used at the hot space. A water jacket outside the cold space was provided and exchanging water at a rate of 22 ml/s. The pressure at the hot space, cold space, and at the output column air space was measured using semiconductor pressure transducer. In our engine, the small pressure difference between the hot space and cold space was neglected. The load of the engine was adjusted using a gate valve at the output column.

In the case of forced vibration experiment, pressurized air was introduced inside the air room of the engine at room temperature using a compressor that is equipped with an automatic timer to monitor the motion of the water columns at various vibration frequency.

5 Results and Discussion

In the calculation, the value of amplitude x_{he}^* is obtained from a given x_{pw}^* . By using the calculated characteristic frequencies, the absolute values and phase lag of the transform functions are obtained and compared with experiments. Under no load condition, that is $C_{pp} = 0$, our calculated values of the characteristic frequencies are 1.15 and 3.39 rad/s.

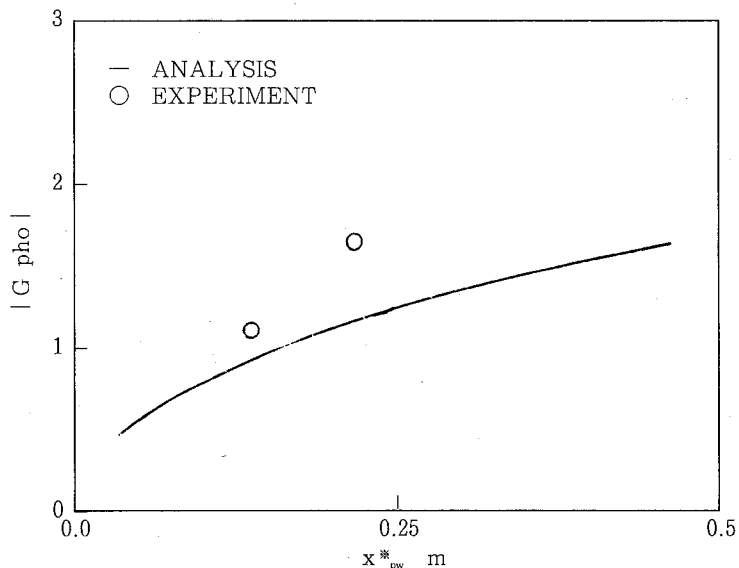


Fig. 3. Frequency transfer function $|G_{pho}|$ vs. amplitude x_{pw}^*

Figures 3 shows that the amplitude ratio $|G_{pho}|$ increases at different amplitude x^*_{pw} . On the other hand, the phase angle of G_{pho} , as shown in Fig. 4, is almost constant.

Figures 5 and 6, respectively, show the behaviour of G_c and its phase angle at different x^*_{pw} .

Table 1. shows the comparison between the experimental and calculation results. It is indicated in the general case, that the calculation results agree well with experiments.

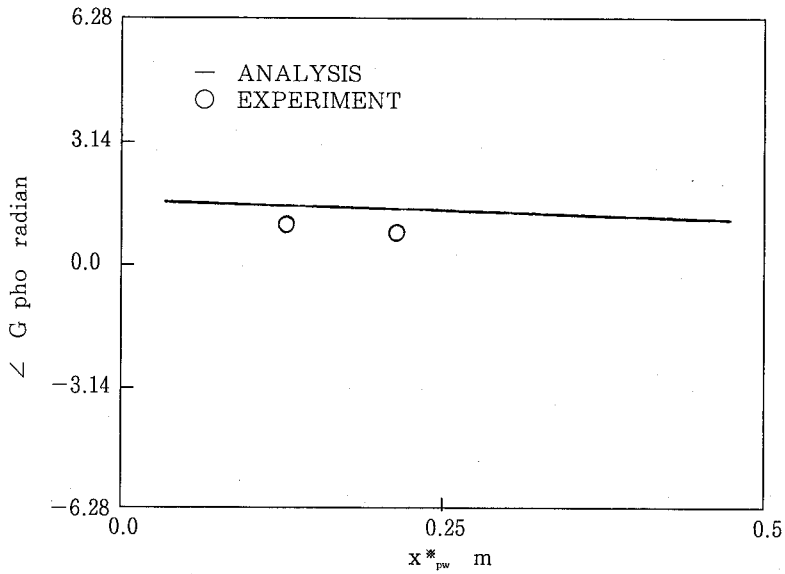


Fig. 4. Phase angle $\angle G_{pho}$ vs. amplitude x^*_{pw}

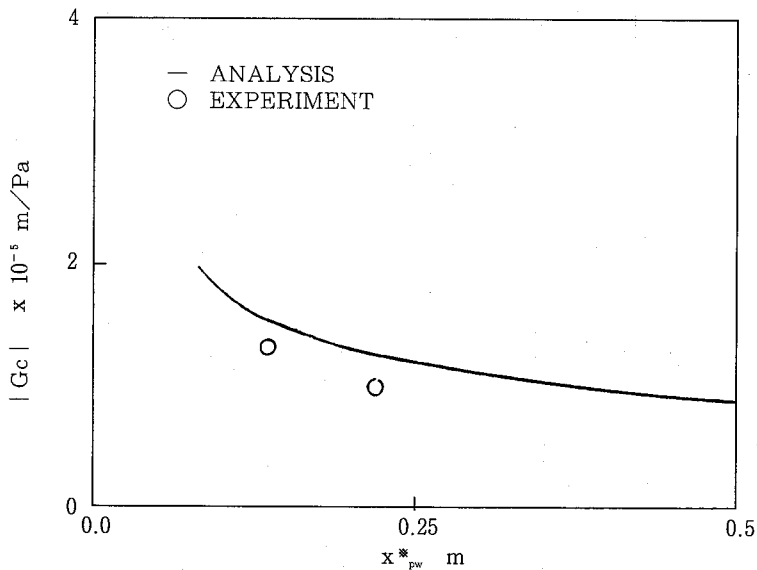


Fig. 5. Frequency transfer function $|G_c|$ vs. amplitude x^*_{pw}

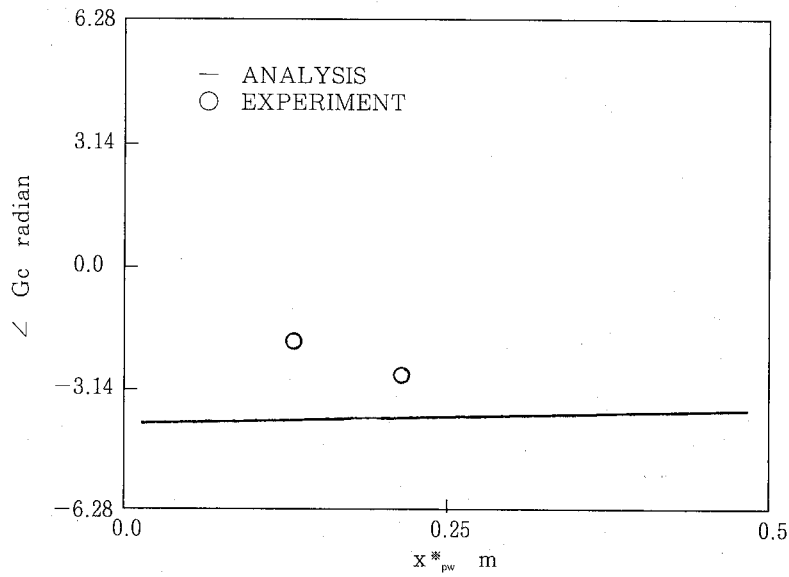
Fig. 6 Phase angle $\angle G_c$ vs. amplitude x_{pw}^*

Table 1. Comparison between experimental and calculation results

Frequency Transfer Function	$x_{pw}^* = 0.13\text{m}$		$x_{pw}^* = 0.21\text{m}$	
	Exp.	Cal.	Exp.	Cal.
$ G_{pho} $	1.12	0.88	1.75	1.1
$ G_s \times 10^{-5}\text{m}/\text{Pa}$	2.03	1.17	2.27	1.17
$ G_o \times 10^{-5}\text{m}/\text{Pa}$	1.72	1.32	1.32	1.07
$ G_y $	1.05	1.19	0.67	1.00
$ G_p $	1.13	1.06	1.20	1.10
$ G_z \times 10^{-5}\text{m}/\text{Pa}$	1.59	1.27	1.04	0.97
Phase Angle	rad		rad	
$\angle G_{pho}$	1.30	1.46	0.89	1.41
$\angle G_s$	-2.03	-3.10	-3.14	-3.11
$\angle G_o$	-2.73	-4.53	-3.45	-4.49
$\angle G_y$	-4.22	-4.37	-4.34	-4.27
$\angle G_p$	-2.92	-2.90	-3.35	-2.86
$\angle G_z$	-0.36	-1.19	0.00	-1.10
Operating Frequency	rad/s		rad/s	
ω_n	3.38	3.39	3.38	3.39

6 Concluding Remarks

The linear analysis presents a clear understanding of the frequency response of the

motion of water columns in liquid piston stirling engine under no load condition. The theory agrees well with experiment.

水ピストンスターリングエンジンの 無負荷における周波数特性

A.M.I. FIGUEROA¹・山崎 堯右²・神山 新一³・岡山 新史¹

(¹ 愛媛大学大学院連合農学研究科施設生産学講座・² 高知大学農学部
生産環境工学科海洋環境工学講座・³ 東北大学流体科学研究所)

要 約

ソーラーやバイオマスのエネルギー利用が可能で維持管理の容易な農業施設灌がい用ポンプとして将来性のある水ピストンスターリングエンジンについて、その液柱振動と加熱室の圧力間の一般的関係を知ることはその特性を予測する上から重要な課題である。

ところで、著者らはそれに関して摩擦などの諸因子を考慮した理論をすでに導いたにもかかわらず、非線形の連立微分方程式のために、実験的に得られた初期値を使った場合のみしかそれらの応答を計算で検討することができず、一般的動特性を理論のみから予測することが出来ず、その性質も明らかでなかった。そこでここでは等価粘性減衰の扱いを取入れ、諸方程式の線形化をはかり、ここで取り扱ったリキッドフィードバックタイプの水ピストンスターリングエンジンの負荷側管端開放時における周波数応答を求め、実験から、ほぼこの扱いが妥当であることを明らかにした。このことから著者らの理論の実用化をはかるための足がかりとした。

References

- 1) West, C.D. : Liquid Piston Stirling Engines, 1 - 121, Van Nostrand Reinhold (1983).
- 2) Reader, G.T., Clarke, M.A., and Taylor, D.R. : Some Experiences with Fluidyne, Proceedings *IMEchE*, 85 - 92 (1982).
- 3) Okayama, S., Yamasaki, T., Kamiyama, S., Kakiuchi, Y., and Figueroa, A.M.I. : On the Oscillation of Three Liquid Columns in a Water-Type Stirling Engine, *Trans. Jpn. Soc. Mech. Eng.*, (in Japanese), **58** (552B), 2380 - 2384 (1992).
- 4) Okayama, S., Figueroa, A.M.I., Kakiuchi, Y., Yamasaki, T., Kamiyama, S., and Yamamoto, M. : Development of Special Water-Hammer Pump with a Water-Type Stirling Engine. *Trans. Jpn. Soc. Mech. Eng.* (in Japanese), **59** (560B), 1134 - 1139 (1993).
- 5) Jacobsen, L.S. and Ayre, R.S. : In Engineering Vibrations with Applications to Structures and Machinery, (Japanese Translation by Gotoh and Kaneda), 221 - 222, Maruzen Co. (1961).
- 6) Hayama, S., Takeda, H., and Mohri, Y. : Resonant Amplitudes of Pressure Pulsation in Pipelines (2nd Report : The Effect of Steady Component of Input Flow on Resonant Amplitudes), *Trans. Jpn. Soc. Mech. Eng.* (in Japanese), **45** (392C), 422 - 430 (1979).

(Manuscript received : September 27, 1993)

(Published : December 27, 1993)

